Stability of solitary waves in finite Ablowitz–Ladik lattices

2002 J. Phys. A: Math. Gen. 35 267

(http://iopscience.iop.org/0305-4470/35/2/307)

INSTITUTE OF PHYSICS PUBLISHING JOURNAL OF PHYSICS A: MATHEMATICAL AND GENERAL

J. Phys. A: Math. Gen. **35** (2002) 267–283 PII: S0305-4470(02)25718-2

Stability of solitary waves in finite Ablowitz–Ladik lattices

P G Kevrekidis[1], I G Kevrekidis[2] and B A Malomed[3]

[1] Department of Mathematics and Statistics, University of Massachusetts, Lederle Graduate Research Tower, Amherst, MA 01003-4515, USA
and
Theoretical Division and Center for Nonlinear Studies, Los Alamos National Laboratory, Los Alamos, NM 87545, USA
[2] Department of Chemical Engineering and Program in Applied and Computational Mathematics, Princeton University, 6 Olden Street, Princeton, NJ 08544, USA
[3] Department of Interdisciplinary Studies, Faculty of Engineering, Tel Aviv University, Tel Aviv, Israel

Received 5 June 2001, in final form 25 October 2001
Published 4 January 2002
Online at stacks.iop.org/JPhysA/35/267

Abstract

We discuss the effects of different types of boundary conditions (b.c.) on the linear stability of a solitary wave in a finite-length dynamical lattice described by the Ablowitz–Ladik (AL) model. Types of b.c. considered are 'fixed' (Dirichlet), no-flux (Neumann) and free as well as periodic b.c. The behaviour of eigenvalues around a stationary nonlinear wave consistent with several types of b.c. is studied analytically and numerically. The translational eigenvalues are found to move away from the origin. It is shown that for b.c. of the 'fixed' type, these eigenvalues bifurcate into a neutrally stable (oscillatory) kind, while the no-flux and free b.c. lead to an exponentially weak instability. The 'rotational' eigenmodes (those related to the gauge invariance of the lattice) strictly remain at the origin, as gauge invariance is not broken by the linear homogeneous b.c. These (numerical) results are compared to the analytical and semi-analytical predictions obtained within the approximation of the images generated by the solitary wave beyond the lattice edges. A potential effect of continuous-spectrum band-edge bifurcations on stability is also evaluated, with the conclusion that that these bifurcations cannot destabilize the 'soliton'. For periodic b.c., the translational invariance is preserved, and so is the Lax-pair structure, sustaining the integrable nature of the problem. The AL model was chosen so that the effects of boundary conditions are monitored in the absence of non-integrable discreteness. Finally, the possibility of the generation of multipulse configurations, due to the interplay of finiteness effects with the exponential tail–tail interaction of the pulses, is examined.

PACS numbers: 05.45.Yv, 02.60.Lj, 05.50.+q

1. Introduction

The problem of boundary conditions is pertinent to all physical as well as computational realizations of mathematical models. In particular, even if one is interested in the properties of the system under study in the infinite domain case, in simulations it is necessary to restrict oneself to a finite domain. It is therefore desirable to understand the effects of domain truncation on features of the problem, with respect to the behaviour of its infinite counterpart.

In practical terms, the issue amounts to understanding the effects of different types of boundary conditions (b.c.) in a class of differential difference equations (DDEs) and/or partial differential equations (PDEs) supporting nonlinear waves. Naturally, many works have attempted to monitor or exploit the effects of b.c. in both parabolic and dispersive equations (see, e.g., [1] and [2] and references therein, respectively), as well as in set-ups that fit into both of them [3, 4]. However, many of the methods used in [1] are quite specific to parabolic systems, while in [2], as is often the case in Hamiltonian set-ups supporting solitary waves, only the dynamics of the waves were examined within adiabatic perturbation theory. On the other hand, studies [3, 4], which dealt with eigenvalue problems under certain b.c., assumed a strong localized perturbation (i.e. the exclusion of a small domain in the two- and higher dimensional problems considered therein). It should also be noted that for kink-bearing systems such as the sine-Gordon equation, the effects of boundary conditions were considered in [5].

The present paper will focus on the stability of a solitary wave interacting with the edges of a finite system. In order to study the stability of the nonlinear wave, we study the eigenvalues of linearization around the stationary solution. In particular, we will try to understand the behaviour of eigenvalues in the Ablowitz–Ladik (AL) model, which is integrable in the limit of the infinite system [6], being the most natural discrete counterpart of the nonlinear Schrödinger (NLS) equation. Note that typical discretization of PDEs, as well as typical DDEs, are non-integrable [7–13], introducing a potential energy barrier (called the Peierls–Nabarro (PN) barrier, following the terminology originally introduced in the theory of dislocations [14]). The interplay of the discreteness and finite-domain boundary conditions, results in an even more complicated behaviour of the system's eigenvalues, which is expected to obscure the finiteness effects proper. This is the reason for choosing (following the pattern of [2]) an example of a discrete system which is integrable in the case of the infinite domain: the integrability avoids complications due to discreteness, as solitons[1] in integrable models *do not* feel the PN potential. The AL equation is

$$\mathrm{i}\dot{u}_n = -(u_{n+1} + u_{n-1})\left(1 + h^2 {u_n}^2\right) + 2u_n \tag{1}$$

where u_n is the complex field at the nth site of the lattice of spacing h, and the overdot stands for the time derivative. We are interested in the soliton solution of equation (1), which has the following form in the infinite system,

$$u_n(t) = \sinh(\omega)\mathrm{sech}\left(\tilde{\omega}(n - \xi)\right)\exp(\mathrm{i}h^2 t) \equiv v_n \exp(\mathrm{i}h^2 t) \tag{2}$$

(the notation follows [15]), where $\sinh(\omega) \equiv \sinh(\tilde{\omega})/h$, $\cosh(\tilde{\omega}) \equiv 1 + h^2/2$. Due to the integrable nature of the AL equation, the parameter ξ in this solution denotes the arbitrary position of the soliton's centre, indicating, as was mentioned above, the effective translational invariance of the solution.

In this paper, we consider the AL lattice containing a large but finite number of sites N, so that $n = 0, 1, \ldots, N + 1$. The boundary conditions are set at $n = 0$ and $n = N + 1$. We deal with four different types of boundary conditions (which pertain to the full perturbed solution):

[1] We will use the term 'soliton' herein with the understanding that we will be discussing the stability of a nonlinear wave which in the case of the infinite domain would be a soliton in the proper sense of the term.

1. Fixed (Dirichlet) b.c.: $u_0 = u_{N+1} = 0$
2. No-flux (Neumann) b.c.: $u_0 = u_2, u_{N+1} = u_{N-1}$
3. Free b.c.: $u_0 = u_1, u_{N+1} = u_N$
4. Periodic b.c.: $u_0 = u_N, u_{N+1} = u_1$.

In all the cases, except for the periodic b.c., the only static state of the soliton possible in the finite lattice is that with the soliton's coordinate ξ taking its value exactly in the middle of the lattice, as otherwise the soliton interacting with the edges of the lattice cannot be in equilibrium. This uniqueness of the static state is a specific feature of the lattice which is integrable in the infinite-length limit, and hence does not give rise to a PN potential, as that potential could create many more bound states of the soliton, not necessarily in the middle of the lattice.

The main objective of the paper is to develop a systematic analysis of the stability of the soliton's static state in the centre of the finite lattice, based on numerical computation of the corresponding linear-stability eigenvalue spectrum. Results will be compared with those produced by less rigorous approaches based on two different versions of the perturbation theory (PT): its adiabatic version, developed in [2], which treats the soliton as a quasi-particle interacting with its two images existing in a virtual form beyond the edges of the lattice, and a more formal singular PT, which will be developed in this paper. The comparison of perturbative results with the (exact, up to numerical precision) numerical results suggests an important conclusion: both versions of PT correctly predict the behaviour of the pair of eigenvalues related to the soliton's translational degree of freedom and both versions lead to an *erroneous* prediction of a bifurcation of a pair of eigenvalues related to the soliton's phase degree of freedom. A cause of the wrong prediction can be easily identified: the picture postulating the interaction of the real soliton with its virtual images introduces a spurious degree of freedom, namely, a phase difference between the soliton and the images. This spurious phase difference gives rise (in the framework of PT) to the predicted bifurcation. Thus, an essential qualitative result of this paper is that it suggests how to distinguish between true and false predictions of PT. This issue is quite important, as PT is frequently the only approach that makes a coherent description of the system possible.

2. The interaction of the soliton with its images

Let us now describe the physical intuition behind effects expected from the boundary conditions. As is well known in physics literature [2], the b.c. can be thought of as generating images of the original pulse. For example, the pulse (2), in conjunction with the b.c. of the 'fixed' type, creates image pulses of opposite sign [2] with their centres located at the points

$$\xi_1 = \xi + L_{\mathrm{fi,r}} \qquad \xi_2 = \xi - L_{\mathrm{fi,l}}. \tag{3}$$

Here, the subscript fi stands for 'fixed', r and l pertaining to the right and left boundaries, respectively. In the case of the 'fixed' b.c., $L_{\mathrm{fi,r}} = 2((N+1) - \xi)$ and $L_{\mathrm{fi,l}} = 2\xi$. Results of calculations are displayed below for $1 < \xi < N$.

The second and third types of b.c. enumerated above can be interpreted in essentially the same way. The no-flux b.c. aim to ensure the vanishing of the discrete derivative at the endpoints of the lattice $(1, N)$, while the free b.c. are equivalent to what may be regarded as vanishing of the derivative at $(1/2, N + 1/2)$. Hence, we expect these two types of b.c. to produce results similar to those described above, with the only exception that $L_{\mathrm{nf}} = L_{\mathrm{fi}} - 1$, $L_{\mathrm{fr}} = L_{\mathrm{fi}} - 1/2$, where the subscripts fr and nf stand for 'free' and 'no-flux' respectively, and the equalities apply to both left and right boundaries. However, the crucial difference of the

second and third types of b.c. from the first type is the fact that the images have the same signs as the original pulse. As has been shown recently [11] (and will also be seen below), this difference in the signs is crucially important for the stability of configurations consisting of the original pulse and its images. In particular, the configuration generated by the 'fixed' type of b.c. is a 'down–up–down' one, in terms of [11], whereas the 'no-flux' and 'free' types of b.c. give rise to an 'up–up–up' configuration ('down' and 'up' stand for the opposite signs in front of the solitary waves). Finally, in the case of periodic b.c., a ring-shaped domain (i.e. a periodic array) is generated, or, in other words, the pulse interacts with its own tail.

If we linearize the AL equation around the solution (2), defining [16]

$$u_n(t) = \exp(\mathrm{i}h^2 t)[v_n + a_n \exp(-\mathrm{i}\lambda t) + b_n \exp(\mathrm{i}\lambda^\star t)] \tag{4}$$

we obtain the following set of equations for the perturbations $\{a_n, b_n\}$,

$$\lambda a_n = -h^2(v_{n+1} + v_{n-1})v_n(a_n + b_n^\star) - \left(1 + h^2 v_n^2\right)(a_{n+1} + a_{n-1}) + (2 + h^2)a_n \tag{5}$$

$$\lambda b_n^\star = h^2(v_{n+1} + v_{n-1})v_n(a_n + b_n^\star) + \left(1 + h^2 v_n^2\right)(b_{n+1}^\star + b_{n-1}^\star) - (2 + h^2)b_n^\star. \tag{6}$$

Equations (5) and (6) constitute an eigenvalue problem, which, if supplemented by appropriate boundary conditions, can be solved numerically. Here * is used to denote complex conjugation. In obtaining equations (5) and (6), it was also used that v_n is a real field.

Prior to probing the effects of the b.c., let us outline the spectral properties of the linear systems (5) and (6) in the case of the infinite lattice, i.e., posed for $-\infty < n < +\infty$. It has four eigenmodes with $\lambda = 0$, two of them being accounted for by the effective translational invariance (with algebraic multiplicity 2 and geometric multiplicity 1, see e.g. [10]), and two others are related to the gauge (phase) invariance of equation (1) under the transformation $u_n \to u_n \exp(\mathrm{i}\theta)$. The latter 'rotational' eigenvalues have the same multiplicities as the translational ones. In addition, there are phonon modes belonging to the continuous spectrum, with $\left(a_n, b_n^\star\right) \sim \exp(\mathrm{i}kn)$, that satisfy the dispersion relation

$$\lambda = \pm[h^2 + 2(1 - \cos k)]. \tag{7}$$

Note that this dispersion relation has *gaps* between the spectral plane origin ($\Lambda = 0$) and the edge of the phonon band, $\lambda_0 = \pm h^2$.

Searching for possible instabilities in a finite AL lattice, we will focus on the (former) zero modes, as, in view of the presence of the above-mentioned gaps, it seems implausible that b.c.-induced bifurcations[2] from the edge of the phonon band can generate an instability. In order for such an instability to arise, the eigenvalues at the edge of the continous spectrum would have to bifurcate from it and cross the distance to the origin in order to exit as an unstable pair of eigenvalues. Note that oscillatory instabilities (in which eigenvalues of the continuous spectrum edge exit in quartets in the complex plane) can be ruled out, at least in the case of a single pulse (see section 4). On the other hand, since the eigenmodes at the origin can bifurcate in either the stable or the unstable eigendirection (even for very small perturbations), they are the most natural potential candidates for the generation of an instability. We will see that the zero modes indeed can, depending on the type of b.c., become unstable, even though the corresponding instabilities are very (i.e. exponentially) weak.

For the first three cases listed above, namely, fixed, no-flux and free b.c., we can predict the behaviour of their crucial eigenvalues on the basis of the pulse-image picture. As is shown in [11, 17], in the quasi-continuum approximation an effective potential of the interaction between far separated pulses is

$$V_{\mathrm{int}}(\xi_1 - \xi_2) \approx V_0 \sigma \exp(-\tilde{\omega}|\xi_1 - \xi_2|) \tag{8}$$

[2] The term bifurcation is used in the text to denote a change in the nature of eigenvalues of the finite domain in comparison with their corresponding position for the infinite domain problem.

where $\xi_{1,2}$ are the coordinates of the pulse centres, V_0 is a positive constant, and $\sigma = -1$ and +1 for the pairs of in-phase (up–up or down–down) and out-of-phase (up–down) solitons, respectively. Note that the quasi-continuum approximation is especially appropriate for the AL model (in comparison with other, non-integrable, discrete models), as it shares the effective translational invariance with the continuum limit. Next, Newton's equations of motion for the centres of mass of the two pulses (considered as quasi-particles parametrized by the positions of their centres of mass in this effective picture), using the interaction potential (8), predict a bound state of the two particles whose eigenvalues can be estimated as

$$\lambda \sim \pm\sqrt{V_{\text{int}}}. \tag{9}$$

Note that by virtue of the definition of the eigenvalues in equation (4), real λ corresponds to stable configurations, while the opposite is true when λ is imaginary. Equation (9) immediately shows that the bound state of unlike (up–down) pulses gives rise to real eigenvalues, hence it is stable, while bound states of like (up–up or down–down) pulses are unstable due to the presence of imaginary eigenvalues. The same result was obtained in [11] for bound states of pulses in the non-integrable discrete NLS model with the on-site nonlinearity.

Taking into account the interaction of a given pulse with its two principal images (the effects of higher order images will only be exponentially smaller in strength as indicated by equation (8) and will thus be ignored in what follows) in the finite-length AL lattice, we expect that the eigenvalues corresponding to the soliton's translational degree of freedom can be estimated as

$$\lambda \sim \pm \mathrm{i}^{(1-\sigma)/2} \exp\bigl(-\tfrac{1}{2}\tilde{\omega}(N + c_{\text{eff}})\bigr) \tag{10}$$

where $c_{\text{eff}} \sim 1$ is an effective correction to the length of the domain generated by the particular b.c. (recall that N is the length of the lattice). As follows from the above expressions for the position of the soliton's images, $c_{\text{eff,nf}} = c_{\text{eff,fr}} - 1/2 = c_{\text{eff,fi}} - 1$. We thus arrive at definite predictions concerning the stability against perturbations of the position of the soliton. In fact, these predictions are the same as those obtained, also by means of the image approximation, in [2].

On the other hand, the 'rotational' symmetry (the gauge invariance) is unaffected by the presence of linear homogeneous boundary conditions, such as those considered in this paper. Hence, we expect that the 'rotational' modes will remain at the origin of the spectral plane (λ_r, λ_i) in the numerical simulations.

3. Numerical results

We will now compare the above predictions for the cases of fixed, no-flux and free boundary conditions with the results of the computer-assisted analysis. We first identify steady-state configurations in the finite-lattice problem in two different ways. First, we merely take a superposition of the original pulse and its (first) images in the infinite lattice, $u_n = U_n \exp(\mathrm{i}h^2 t)$, where $U_n = v_n + w_n$, with v_n given by equation (2) and

$$w_n = \begin{cases} \pm\epsilon \sinh(\omega)\operatorname{sech}(\tilde{\omega}(n - \xi_1)) & \xi \leqslant n \leqslant N \\ \pm\epsilon \sinh(\omega)\operatorname{sech}(\tilde{\omega}(n - \xi_2)) & 1 \leqslant n < \xi \end{cases} \tag{11}$$

with ξ_1, ξ_2 given by equation (3) in the case of fixed b.c., or similar values defined above for other types of b.c. The minus and plus signs in equation (11) pertain to the fixed and no-flux/free b.c., respectively. The amplitude ϵ introduced in equation (11) is actually 1, but we have opted to put it there to stress the fact that w_n, considered within the domain of interest ($1 \leqslant n \leqslant N$), is a small perturbation. In view of this, terms of higher orders

(such as containing ϵ^2) with respect to this small perturbation will be neglected in the leading-order approximation. The ansatz (11) provides an approximate description of the bound state formed by the original solitary wave and its principal images. It should be noted, however, that this ansatz also generates an 'extraneous' degree of freedom which corresponds to the relative phase of the solitary wave and its images.

When constructing the above ansatz, the value of the coordinate ξ of the centre of the (main) soliton in the expression (2) is taken exactly in the middle of the finite lattice, as it is evident that, due to its interaction with the edges (or, in other words, with its images), the soliton will only have one equilibrium position (stable or unstable) in the middle of the lattice. Note that for models of other types, which are not integrable in the infinite-lattice limit, the above-mentioned PN potential may give rise to a large number of other equilibrium positions, provided that the lattice is long enough [2]. However, the exceptional feature of the AL (integrable) lattice is, precisely, the absence of the PN potential, hence the equilibrium position for the soliton may be found solely at the centre of the finite lattice.

A direct numerical approach was also employed in seeking the bound state. This approach involved the solution of the stationary version of equation (1) on the finite lattice by means of Newton iterations. The initial approximation was taken as the infinite-lattice soliton (see equation (2)) placed at the centre of the finite domain. The results obtained in this way for a typical case and for fixed b.c. are presented in figure 1. The top panel shows the difference between the numerically exact solution for the finite lattice and its infinite-lattice counterpart is given by equation (2). Markedly, the (symmetric, as per our choice of initial condition) error is larger near the boundary. The bottom panel shows the difference between the same numerically exact solution produced by the Newton iterations and the ansatz-based soliton–image solution ($U_n \equiv u_{IM}$). It should be noted that the soliton–image solution is constructed by finding ξ for the exact solution (computed via the Newton), then finding the corresponding ξ_1, ξ_2 using equation (3) and finally obtaining the correction w_n via equation (11). It can clearly be seen that the addition of the images drastically improves the accuracy of the analytical approximation. It can also be observed that, in the latter case, the L^∞ norm of the error is much less than when using the infinite-lattice soliton as the approximation. Nevertheless, as we will see below, this ansatz-based approach should sometimes be used with caution.

Figure 2 shows for fixed b.c. the behaviour of the translational and 'rotational' eigenvalues as a function of the total length of the lattice L (which is exactly the same as the total size N used above). The corresponding data, obtained from direct numerical solution of the linear eigenvalue problem, are shown, respectively, by circles connected by the solid line and stars connected by the dashed line. The panels show the eigenvalues of small perturbations around the ansatz-based solution (using the approximation of equation (11)) and the numerically exact solution obtained by the Newton iterations. The following conclusions can be drawn:

- There is an excellent fit of the translational eigenvalue's dependence on the domain length L to an exponential dependence predicted by the image-ansatz approximation.
- We can observe where (and why) the image-ansatz approximation fails and where it succeeds. The approximation correctly captures the bifurcation of the translational modes. However, it also predicts that the 'rotational' modes will bifurcate by a similar amount. This prediction (which will also be analytically justified below) is of course in contrast with the full numerical result. The latter finds the 'rotational' eigenvalues to be below the numerical precision and hence we can conclude that, as is suggested by the persistence of the gauge invariance of the full problem when including the linear homogeneous b.c., they remain at the origin of the spectral plane. One may attribute this failure to the 'creation' (by the ansatz) of an extraneous degree of freedom, which is the relative phase between

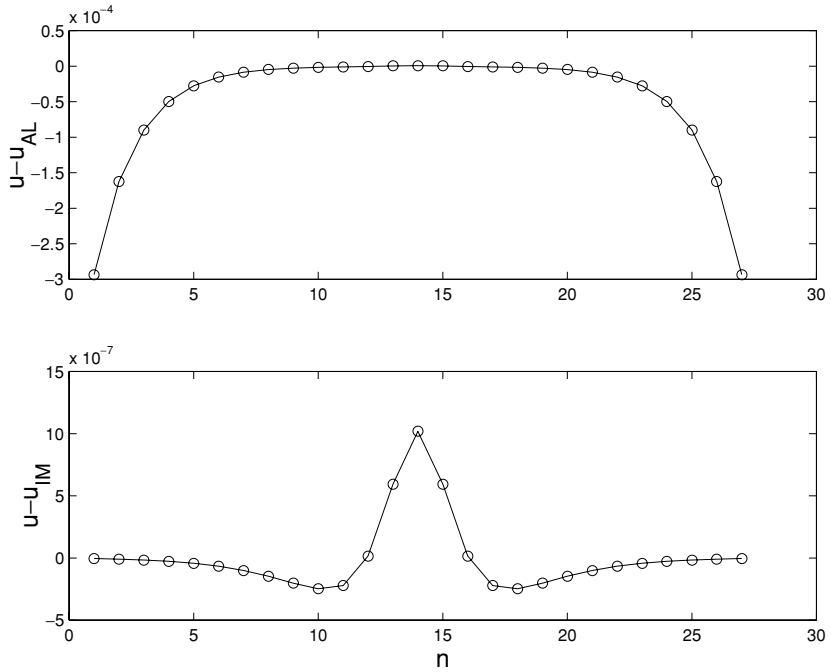

Figure 1. For the 'fixed' b.c., the difference between the numerically exact solution u and the infinite-lattice soliton u_{AL} is shown in the top panel for a finite lattice with $N = 27$. The bottom panel shows the difference between the numerically exact solution u and the soliton–image ansatz $u_{IM} \equiv U_n$ (cf section 3) for the same lattice. Notice the significant difference in the scales of the difference (10^{-4} in the top panel versus 10^{-7} in the second one).

the solitary wave and its image. The gauge invariance is destroyed by the variation of this extra degree of freedom, which yields nonzero 'rotational' eigenvalues even though the nature of the boundary conditions does not sustain such behaviour. Hence, we conclude that the approximation is useful in revealing the behaviour of the translational modes, but it should not be trusted in the treatment of the 'rotational' eigenmodes.

- The bifurcation of the pair of translational eigenmodes in this case takes place along the real axis in the complex plane of the eigenvalue λ (defined in equation (4)), thus giving rise to a stable configuration. This result is in agreement with [11], according to which the bound states of pulses with opposite parity are (neutrally) stable, and it also agrees with the phenomenology of [2], where oscillatory behaviour is observed for fixed b.c. (see, e.g., figure 2 in [2]). It should be noted that the (erroneous) prediction for the 'rotational' modes of the image approximation to the exact solution is that they bifurcate in the opposite direction, giving rise to an (exponentially weak) *spurious* instability.
- In figure 3, we show the slope of the semilog plot from figure 2 (for the translational eigenvalues) versus the solitary wave's inverse width $\tilde{\omega}$, which is defined in equation (2). The theoretical prediction following from equation (10) is that the slope of this new plot is $-1/2$. The numerical result for the slope is -0.501, in excellent agreement with the theoretical prediction. Note that the pre-exponential dependence of λ on $\tilde{\omega}$ (i.e. the point where the semilog plot intersects the vertical axis in figure 1) determines the value of the constant c_{eff} from equation (10) for a specific set of b.c. (see details below).

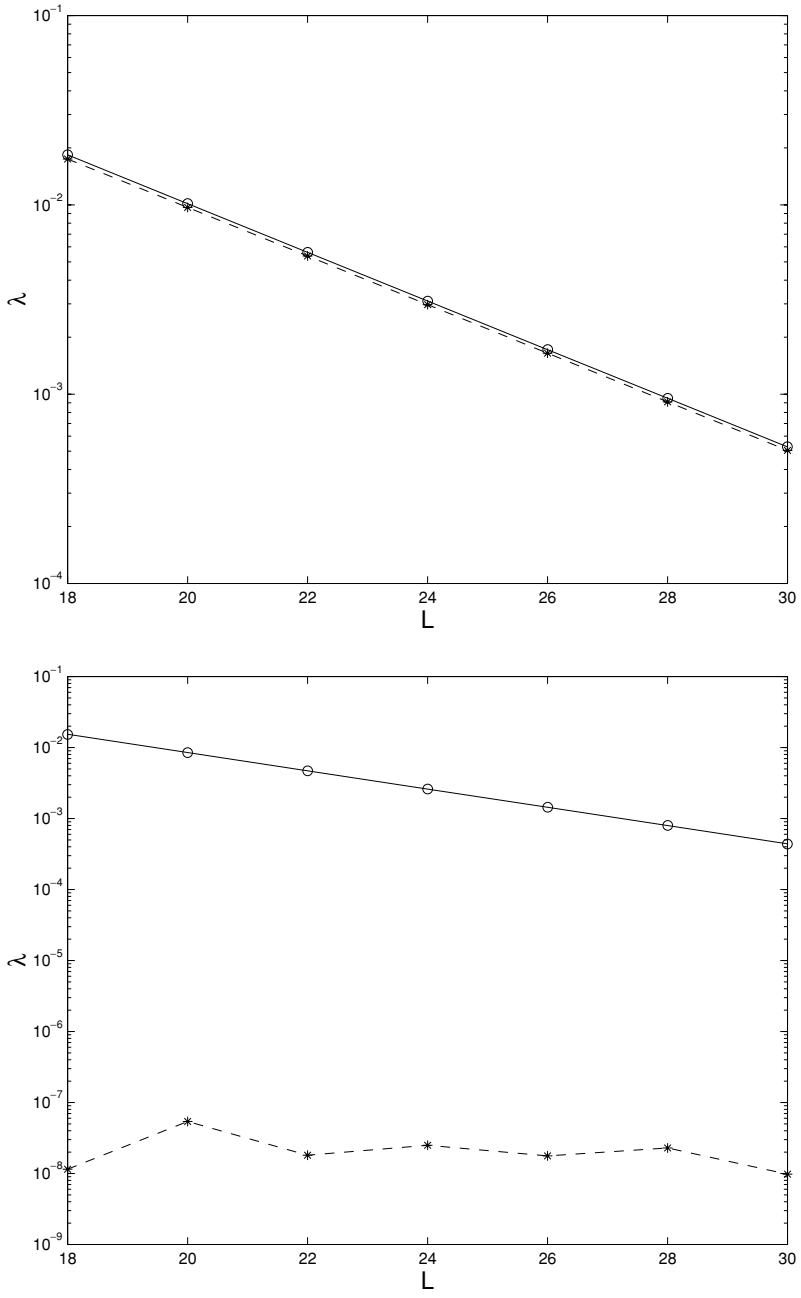

Figure 2. The top panel shows the behaviour of the translational eigenvalues (data points denoted by circles and connected by a solid line) and the 'rotational' eigenvalues (data points denoted by stars and connected by a dashed line) as a function of the lattice size L for perturbations around the solutions obtained through the image-ansatz approximation. This behaviour is to be compared/contrasted with the bottom panel, which shows the behaviour of the translational and 'rotational' eigenvalues (with the same notation) for perturbations around the numerically exact solution obtained by the Newton iterations. Both plots pertain to 'fixed' b.c.

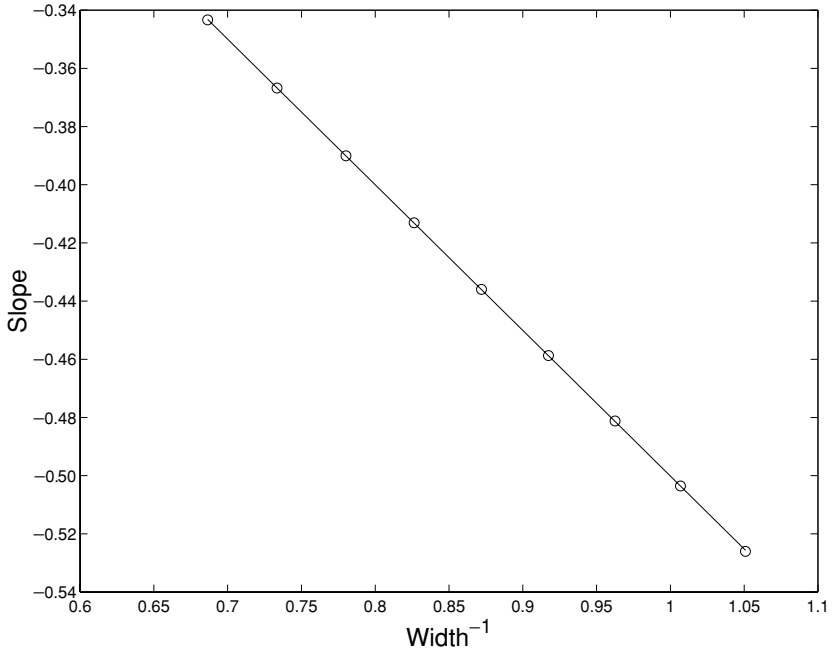

Figure 3. The slope of the plot in figure 2 plotted against the inverse width $\tilde{\omega}$ of the soliton for b.c. of the 'fixed' type.

Now, we will display numerical results for the no-flux and free b.c. and compare them with those for b.c. of the 'fixed' type. As may be expected, the results for these two types of b.c. are essentially the same and will be presented together in what follows. The only difference between them is the value of c_{eff}, which will be highlighted in the last item of the list below.

- In this case the translational pair of eigenmodes bifurcates along the imaginary axis of the spectral plane, giving rise to an exponentially weak instability (cf equation (4)). This conclusion is once again in agreement with the results of [11], which state that configurations of pulses with the same parity ('up–up' pulses) are unstable, as well as with figure 4 of [2]. Additionally, the image–ansatz approximation predicts a spurious 'rotational' eigenvalue pair bifurcation along the real axis of the plane, while the preservation of gauge invariance by the b.c. precludes such a bifurcation for the *exact* solution.
- Performing the procedure which produced figure 3 in the previous case, i.e. finding the slope of the dependence of λ on L (for the translational eigenvalues) for different values of the widths $\tilde{\omega}$, and plotting it versus $\tilde{\omega}$, we obtain once again the best-fit slope -0.500 for the no-flux b.c., and -0.499 for free b.c., in excellent agreement with the $-1/2$ theoretical prediction based on equation (10).
- Finally, comparing the effective corrections to the system's size for the different types of b.c., we find $c_{\text{eff,fr}} - c_{\text{eff,nf}} = 0.527$, which should be compared with the above theoretical prediction which yielded the value $1/2$ for the same quantity, and $c_{\text{eff,fi}} - c_{\text{eff,nf}} = 1.001$, to be compared with the theoretically predicted value 1.

In closing this section presenting our numerical results, let us note that an alternative methodology for obtaining the bifurcations of the relevant eigenvalues would be to consider

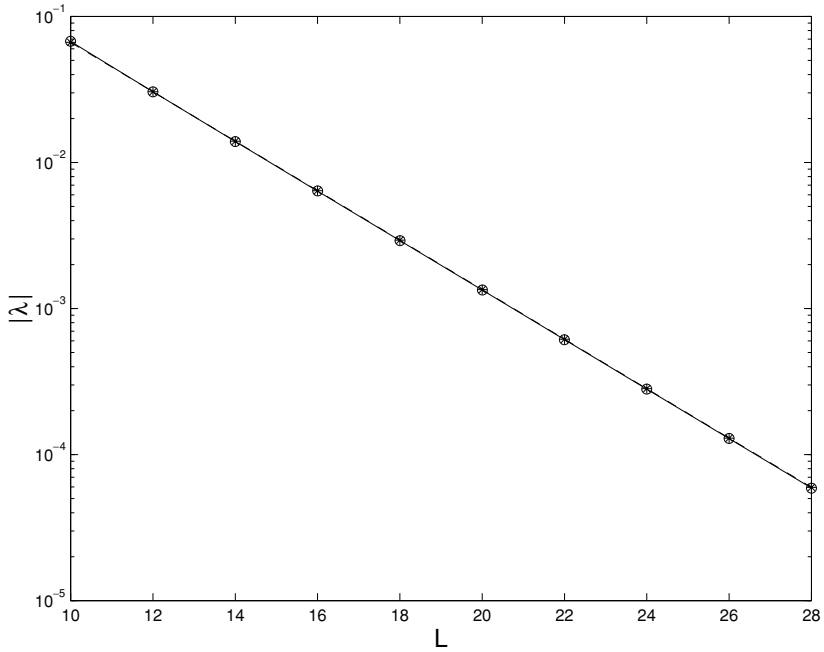

Figure 4. Numerical results for the bifurcation of the translational modes at $h = 0.7$ (the circles denote individual numerical data points and are connected by the solid line) as compared with the theoretical prediction (the stars denote the theoretical prediction for the values of L for which the numerical experiments were performed and are connected by the dashed line) based on equation (25). The two lines are practically indistinguishable.

a two-pulse configuration in a box of size $2L$ (or a three-pulse configuration in a box of size $3L$) with periodic boundary conditions. This method has been used in [18]. It has the advantage of capturing the most important contribution to the bifurcating eigenvalue pair without introducing spurious bifurcations. On the other hand, it has the disadvantage that *only* eigenvalues whose eigenfunctions obey a specific symmetry requirement will be relevant for the problem of the single pulse in the domain of size L. In particular, for a single pulse there are four eigenvalues near the origin of the spectral plane, while for two pulses the corresponding eigenvalues will be eight. Two of them will be the phase modes, while from the remaining six, only the non-zero eigenvalues satisfying the appropriate (spatial profile) symmetry requirement will be relevant for the problem of a single pulse in a domain of length L. Due to the latter complication and as per the exponential nature of the corrections to leading order effects (as well as per the very good agreement of the above presented analysis with the numerical results), we do not pursue this method here.

4. The singular perturbation theory

Even though many of the results and conclusions presented above have already been qualitatively and, in part, even quantitatively justified, in this section we give an outline of a singular perturbation method for determining the eigenvalue bifurcations, as an alternative to the image-based approximation, that reduced the dynamics to a few degrees of freedom representing the centres of the pulse and its images, as illustrated by equations (8)–(10).

Using the notation $a_n \equiv f_n + g_n$ and $b_n \equiv f_n - g_n$ for the perturbations introduced in equation (4) [16, 19], we can rewrite the linear stability problem as [10]

$$\mathrm{i}\lambda g_n = -L_- f_n \tag{12}$$

$$\mathrm{i}\lambda f_n = L_+ g_n \tag{13}$$

where the operators L_- and L_+ are defined as [10]

$$L_- f_n = (f_{n+1} + f_{n-1})\left(1 + h^2 U_n^2\right) - (2 + h^2) f_n \tag{14}$$

$$L_+ g_n = (g_{n+1} + g_{n-1})\left(1 + h^2 U_n^2\right) - (2 + h^2) g_n + 2h^2 U_n (U_{n+1} + U_{n-1}) g_n. \tag{15}$$

In these equations, U_n is the (time-independent part of the) solitary wave spatial profile, which in the infinite domain coincides with v_n (see equation (4)). In order to capture the solution in the case of the bounded domain, we use the picture set forth by the physical intuition, assuming the creation of the images, as was also done in [2]: we set $U_n \equiv v_n + w_n$, where v_n is the exact soliton solution defined as per equation (2), and w_n is given by equation (11). With that in mind, we can now rewrite the set of eigenvalue equations (12) and (13) as

$$\lambda^2 = \langle L_+ f_n | L_- f_n \rangle \tag{16}$$

where the angular brackets are used to form the inner product which is necessary in order to derive an equation for the eigenvalues.

The unperturbed eigenvalue problem has a solution with $\lambda = 0$ and $f_n = v_n$. The perturbed eigenvalue problem, with $U_n = v_n + w_n$ in the expressions for the operators L_-, L_+, no longer has $f_n = v_n$ as its zero-mode solution, since the phase modes are now bifurcating (in the image-based approximation). The solvability condition of the singular perturbation theory gives a correction to the zeroth-order ($\lambda = 0$) eigenvalue, by projecting the new eigenvector f_n onto its unperturbed predecessor, namely v_n (see, e.g., [19]). Hence, the solvability condition now reads

$$\lambda^2 = \langle L'_+ v_n \mid L'_- v_n \rangle. \tag{17}$$

We use the prime in the operators to indicate that in the latter case $U_n = v_n + w_n$, rather than $U_n = v_n$, as was the case before.

Using the fact that $L_- v_n = 0$, we obtain

$$L'_- v_n = 2\epsilon h^2 v_n w_n (v_{n+1} + v_{n-1}) + \mathrm{O}(\epsilon^2) \tag{18}$$

while

$$L'_+ v_n = 2h^2 v_n^2 (v_{n+1} + v_{n-1}) + \epsilon h^2 \left[2v_n^2 (w_{n+1} + w_{n-1}) + 4w_n (v_{n+1} + v_{n-1}) v_n\right] + \mathrm{O}(\epsilon^2) \tag{19}$$

hence the leading order ($\mathcal{O}(\epsilon)$) contribution to λ^2 is given by

$$\lambda^2 = 4\epsilon h^4 \left\langle v_n^2 (v_{n+1} + v_{n-1}) \,\middle|\, v_n w_n (v_{n+1} + v_{n-1}) \right\rangle. \tag{20}$$

A key feature is the linear dependence of the expression (17) on w_n, which implies that the minus sign for the 'fixed' type of b.c. in equation (11) lends the phase eigenmode an imaginary eigenvalue λ (since all other quantities are positive), hence it is unstable, exactly as revealed by the numerical computations presented above. In contrast to this, the plus sign corresponding to the no-flux and free b.c. in equation (11) leads to real λ, hence a stable phase eigenmode, once again in agreement with the numerical results obtained for the perturbations around the image-based ansatz. We should remind the reader, however, that this is a *spurious* bifurcation since for the finite domain with linear homogeneous b.c., the phase invariance is preserved.

Turning now to the translational modes, the eigenvalue equations (12) and (13) may be written as

$$\lambda^2 g_n = \langle L_- g_n L_+ g_n \rangle. \tag{21}$$

The appropriate eigenvector of the unperturbed system corresponding to $\lambda = 0$ is $g_n = \partial_\xi v_n$. Using once again primes in the operators to denote the perturbed problem, we can derive the solvability condition,

$$\lambda^2 = \langle L'_- \partial_\xi v_n L'_+ \partial_\xi v_n \rangle. \tag{22}$$

Using the fact that $L_+ \partial_\xi v_n = 0$, we conclude that

$$L'_+ \partial_\xi v_n = 2\epsilon h^2 [v_n (w_{n+1} + w_{n-1}) \partial_\xi v_n + 2 w_n v_n (\partial_\xi v_{n+1} + \partial_\xi v_{n-1})] + \mathrm{O}(\epsilon^2) \tag{23}$$

while

$$L'_- \partial_\xi v_n = -2h^2 v_n (v_{n+1} + v_{n-1}) \partial_\xi v_n. \tag{24}$$

Combining equations (23) and (24), we obtain

$$\lambda^2 = -4\epsilon h^4 \langle v_n (v_{n+1} + v_{n-1}) \partial_\xi v_n | (v_n (w_{n+1} + w_{n-1}) \partial_\xi v_n + 2 w_n v_n (\partial_\xi v_{n+1} + \partial_\xi v_{n-1}) \rangle. \tag{25}$$

Note that the asymmetry between the operators L'_- and L'_+ gives rise to the extra minus sign in equation (25), as compared to equation (20). Along with the positivity of terms involving v_n and the linear dependence on w_n, this leads us to the conclusion that, in the present case (i.e. for the soliton-image ansatz), the pair of translational eigenvalues bifurcates in a direction orthogonal to that of the phase eigenvalues, exactly as observed in the numerical computations outlined in the previous section. The similarity between the expressions for the two different sets of the eigenmodes justifies the observation that the bifurcation of the two modes takes place at the same order for all three different types of b.c. within the framework of the image-ansatz approach. Furthermore, we conclude that, due to the form of the expressions in equations (20) and (25) (namely, the expressions are real, thanks to the nature of the relevant operators), the result for λ^2 is always real, hence the bifurcations may only take place along the real and the imaginary axes, and no quartets of eigenvalues can appear, thus no oscillatory (Hopf-like) instabilities occur [20–22].

It should be noted that this conclusion also pertains to bifurcations of modes from the edges of the phonon spectrum. In this work, we did not consider such bifurcations (which were studied in [10, 19, 23–25]) in detail for a good reason. Indeed, as corrections to the edge eigenvalues are real (for reasons similar to those explained above), and since they are small corrections $\sim \exp(-\tilde{\omega} L/2)$ to the band-edge eigenvalues, which are separated by the above-mentioned gaps from the origin of the spectral plane (see equation (7)), it is obvious that, on the one hand, there is no 'danger' of oscillatory instabilities, and on the other, bifurcations with small values of control parameters considered here cannot pull the eigenvalue across the finite spectral gap so that it would pass through the origin (as needed in order to generate an instability).

A general conclusion suggested by this discussion is that, when studying the effects of b.c. on the stability of a soliton in a Hamiltonian system with a gap in its linearization spectrum, one needs, for small perturbations (i.e. for $L \gg \tilde{\omega}^{-1}$), to account only for eigenvalues bifurcating from the origin of the spectral plane. The theoretical prediction given by equations (20) and (25) can be compared to the numerical results, which is done in figure 4 for the translational eigenmodes and b.c. of the 'fixed' type. The solid line connecting the circles standing for numerical data points shows the semilog dependence of the translational modes' eigenvalues for $h = 0.7$ as obtained from the numerical computations, and the dashed line connecting the stars (selected data points for the same total lattice lengths as in the numerical experiments)

shows the theoretical prediction based on equation (25). We see that the two dependences are practically indistinguishable. In the evaluation of the inner products in equation (25), only the contributions from $n = 1, \ldots, N$ were included in the summation. Hence for the translational modes, the singular perturbation theory in conjunction with the image approximation works very well. For the phase modes, on the other hand, the image method provides, in equation (20), w_n such that $L'_- U_n \neq 0$, even though the preservation of the symmetry for the numerically exact solution generated by the Newton iterations leads to $L'_- U_n = 0$, as is also verified by the bottom panel of figure 2.

5. Periodic boundary conditions

The last type of boundary conditions which we aim to briefly examine are periodic b.c. As before, the 'rotational' invariance is not affected by this type of b.c. On the other hand, as is discussed in [26], the periodic b.c. restore the translational invariance of the infinite-lattice problem. The most illustrative way to see this is to consider the system with the periodic b.c. as representing a ring. On the ring, it neither matters where the 'end-point' of the lattice is formally located, nor does it matter where the solitary wave is centred. Hence, the restoration of the translational invariance preserves the translational eigenvalues at the origin, which makes the finite lattice 'as close as may be' to the infinite one. The only difference between the two, which clearly does not affect soliton stability, is that the continuous spectrum, instead of forming a continuous band, has only a finite (equal to the lattice size) number of eigenmodes.

The well-known study [27] on the integrability of the Korteweg–de Vries equation with periodic b.c. strongly suggests that the finite AL with periodic b.c. shares the integrability of its infinite counterpart. In fact, one can show [28] that the Lax-pair structure of the original infinite lattice [6] is preserved by the periodic b.c. and hence the model should be integrable.

An alternative and perhaps more intuitive way to show the integrability of the finite-lattice AL model with periodic b.c. would be to use a method of [15] as follows: one can demonstrate that the stationary version of the model has the property that $H_1 = H_2 = \cdots = H_N$, where $n = 1, \ldots, N$,

$$H_n = v_{n-1}^2 v_n^2 + h^{-2}\left[v_{n-1}^2 + v_n^2 - 2\left(1 + \frac{h^2}{2}\right) v_n v_{n-1}\right]$$

and the appropriate adjustments are made at the boundary, i.e. $v_0 = v_N$. Hence, these N quantities are independent of n and they may be constants of the motion, making this system with N degrees of freedom integrable. When temporal dynamics is added to the model, the conservation laws can be written in the form $\partial T_n/\partial t + \Delta_n H_n = 0$ with appropriately defined T_n (and $\Delta_n H_n = H_{n+1} - H_n$), hence integrability will be preserved [15].

6. Multiple pulses

As noted in section 3, the competition between the two exponential dependences on the distance from the corresponding boundaries can give rise (for a single pulse) to only one stable or unstable fixed point, namely the one at the centre of the finite domain in the framework of the AL model.

However, in the same spirit as in [11, 30], one may expect to obtain multipulse configurations in this model. In the case of [11, 30], the multipulses resulted from the interplay between the periodic discreteness-induced force and the exponential tail–tail interaction between the pulses. In the present framework, they will be the result of the much more delicate balance between the exponential pulse–boundary interaction (exponential

in the distance of the pulse from the boundary) and the exponential tail–tail interaction between the multiple pulses inside the domain. The latter situation is much more special as it will result in only one additional fixed point, as opposed to multiple fixed points that, for instance, the presence of a PN barrier (and its competition with the tail–tail interaction) would produce. In what follows, we consider this possibility in the framework of perturbation theory. For more than two pulses (in the finite domain), the considerations given below can be generalized in a straighforward manner to obtain the relevant additional fixed points corresponding to stationary multipulse configurations.

The configuration with two AL solitons in a finite lattice is quite similar, due to the absence of the Peierls–Nabarro potential, to the case when two solitons are created in a finite NLS system with the same b.c. as in its AL counterpart. If the distances of the solitons from the nearest edge are $L_{1,2}$, and each soliton is taken in the form

$$u_{1,2}(x,t) = \eta \mathrm{sech}(\eta(x-\xi_{1,2}))\exp\left(\tfrac{1}{2}\mathrm{i}\eta^2 t + \mathrm{i}\phi_{1,2}\right) \tag{26}$$

an effective potential of the interaction of the two solitons with each other, and also with their images, is

$$U(L_1, L_2, \phi) = \mathrm{const}\cdot\left[\mathrm{e}^{-2\eta L_1} + \mathrm{e}^{-2\eta L2} - \cos\phi\,\mathrm{e}^{-\eta(L-L_1-L_2)}\right] \tag{27}$$

where the 'fixed' b.c. are implied, $\phi \equiv \phi_1 - \phi_2$ is the phase shift between the solitons (the amplitudes of both solitons are of course assumed equal), and the constant is positive. Note that the considerations can easily be generalized to the cases of no-flux and free boundary conditions, in accordance with the previous sections.

As follows from expression (27), there is an equilibrium state of the system with

$$L_1 = L_2 = \tfrac{1}{4}[L - (\ln 2)/\eta] \qquad \phi = \pi. \tag{28}$$

It is easy to check, and is actually obvious without any calculation, that the state (27) provides for a local minimum of the potential relative to variations of $L_{1,2}$, and a local maximum of the potential relative to the variation of ϕ. Because, as is known, an effective mass related to the positional degree of freedom of an NLS soliton is positive, while an effective mass corresponding to the relative phase is *negative* [29], these results suggest that the equilibrium state (28) is stable.

Note that, being guided by the previously obtained results, we should *not* analyse the stability of this equilibrium state against variations of the extraneous degree of freedom in the form of the phase differences between each soliton and its image.

To complement these analytical predictions, we tracked down such a two-pulse by means of numerical computation. Two examples of such configurations are shown in figure 5. We have found generically that these configurations exist and *can* be stable (as can be verified by the bottom panel of the figure showing a configuration on a lattice of $N = 23$ sites). This is contrary to what happens for smaller lattices (or for smaller values of the lattice spacing for which in our model the phonon spectrum band edge approaches the origin of the spectral plane); in the latter case, it is quite generally found that collision of two pairs of eigenmodes with opposite Krein signature [16, 21, 30, 31] will result in a Hamiltonian Hopf bifurcation (see e.g. the top panel of figure 5).

Similar considerations can naturally be generalized to multiple pulse settings not only for the AL model, but also for the continuum NLS equation. Note that this novel and delicate suggested interplay between finiteness and tail–tail interaction can lead to steady-state configurations that would not be present for the infinite domain problem.

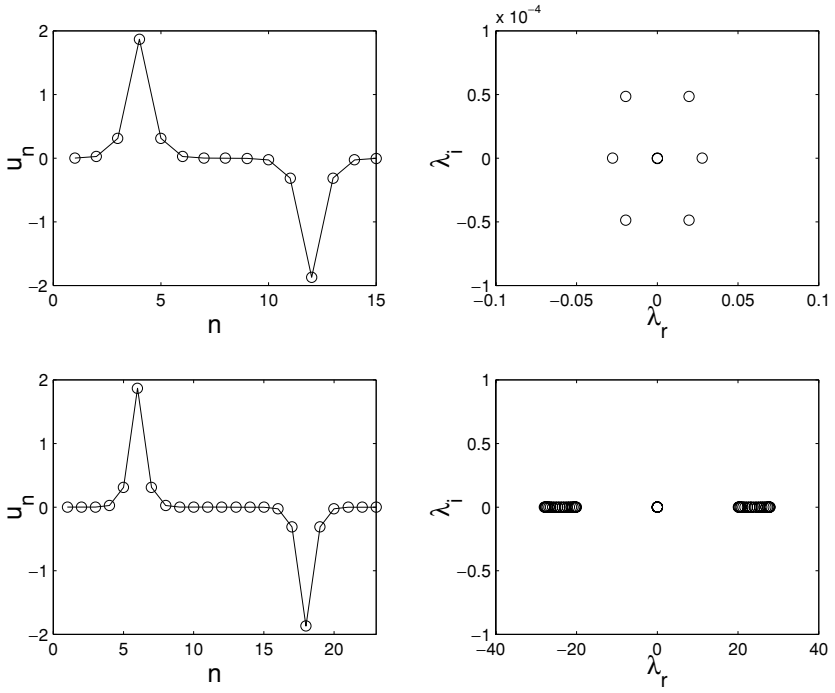

Figure 5. The top panel shows an unstable configuration (top left subplot) for a small lattice of $N = 15$ sites. Here $h = \sqrt{10}$. The top right panel shows a blow-up of the corresponding spectral plane picture of the linear stability analysis around the configuration of the top left panel. Clearly discernible is a quartet of eigenvalues signalling the presence of an oscillatory instability. On the other hand, for a larger lattice of $N = 23$ (for the same spacing) a stable configuration is shown in the bottom left panel, as is verified by all of the corresponding eigenfrequencies of the bottom right panel being real. Both numerical experiments have been performed for fixed boundary conditions.

7. Conclusions

The objective of this paper was to reconsider the stability of solitons in long but finite discrete dynamical lattices, and to compare it with the stability of their infinite counterparts. We have restricted the analysis to discrete versions of the nonlinear Schrödinger equation in one spatial dimension, examining effects of different types of boundary conditions. The effective translational invariance of the AL model in the infinite lattice is broken by the b.c., except for the case of the periodic b.c. Due to the absence of the Peierls–Nabarro potential in the AL lattice, the only static soliton possible in the finite lattice (except for the case of the periodic b.c.) is located exactly in the middle of the lattice. A linear-stability analysis of this static solution demonstrates that exponentially small (in the lattice size) finite translational eigenvalues bifurcate from the origin. The bifurcation yields a (neutrally) stable pair of eigenmodes for the boundary conditions of the 'fixed' type, and an unstable pair in the case of no-flux and free boundary conditions. The phase symmetry (gauge invariance) being preserved by the boundary conditions, the corresponding eigenvalues must stay at the origin.

We have compared the above-mentioned stability results with those produced by the heuristic (adiabatic) perturbation theory (PT) earlier developed in [2], which treats the AL soliton as a quasi-particle interacting with its images, as well as with results produced by a more formal singular PT. We concluded that both versions of the PT correctly describe the emerging

translational eigenvalues and their stability character, but they both produce *erroneous* results for the phase eigenvalues: PT predicts the appearance of finite (i.e., nonzero) phase eigenvalues due to *spurious* degrees of freedom in the form of the phase difference between the soliton and its images. In fact, this conclusion, which makes it possible to distinguish between true and spurious results to be expected from PT, is an important qualitative result of this paper. We also mention that PT correctly predicts some other important features of the stability problem, such as the non-existence (in the single-pulse case) of a bifurcation generating a quartet of complex eigenvalues, and the absence of an instability due to band–edge bifurcations from the continuous spectrum.

It should also be noted that our results can naturally be generalized in the case of mixed boundary conditions. For instance, it follows from our considerations that if mixed boundary conditions of fixed and free (or no-flux) are used in the two different boundaries, that preferential motion of the solitary wave will occur in one direction (since one of its images is attracting the wave while the other is repelling it). In that case, no fixed point (stationary configuration) will be present. If, on the other hand, free and no-flux boundary conditions are used in the two edges, the considerations will be the same as if either free or no-flux b.c. had been applied to both boundaries but the ensuing unstable fixed point will be slightly displaced from the centre of the domain due to the slight asymmetry (by half a lattice spacing) of the corresponding images.

We believe that the nature of the results obtained in this paper, as well as the qualitative arguments presented herein, should be immediately generalizable to more complicated models.

Acknowledgments

We appreciate useful discussions with D J Kaup, C Muratov and T Kapitula.

References

[1] Sandstede B and Scheel A 2000 *Physica* D **143** 233
[2] Rasmussen K Ø, Cai D, Bishop A R and Grønbech-Jensen N 2000 *Phys. Rev.* E **55** 6151
[3] Ward M J and Keller J B 1993 *SIAM J. Appl. Math.* **53** 770
[4] Ward M J, Henshaw W D and Keller J B 1993 *SIAM J. Appl. Math.* **53** 799
[5] De Leonardis R M, Trullinger S E and Wallis R F 1980 *J. Appl. Phys.* **51** 1211
[6] Ablowitz M J and Ladik J F 1975 *J. Math. Phys.* **16** 598
[7] Peyrard M and Kruskal M D 1984 *Physica* D **14** 88
[8] Boesch R and Willis C R 1988 *Phys. Rev.* B **38** 6713
[9] Kevrekidis P G, Jones C K R T and Kapitula T 2000 *Phys. Lett.* A **269** 120
[10] Kapitula T and Kevrekidis P G 2001 *Nonlinearity* **14** 533
[11] Kapitula T, Kevrekidis P G and Malomed B A 2001 *Phys. Rev.* E **63** 036604
[12] Kevrekidis P G and Weinstein M I 2000 *Physica* D **142** 113
[13] Cai D, Bishop A R and Grønbech-Jensen N 2000 *Phys. Rev.* E **53** 4131
[14] Hirth J P and Lothe J 1982 *Theory of Dislocations* (New York: Wiley)
[15] Ablowitz M J and Herbst B M 1993 *Important Developments in Soliton Theory* ed A S Fokas and V E Zakharov (New York: Springer)
[16] Johansson M and Aubry S 2000 *Phys. Rev.* E **61** 5864
[17] Afanasjev V, Malomed B and Chu P 1997 *Phys. Rev.* E **56** 6020
[18] Or-Guil M, Kevrekidis I G and Baer M 2000 *Physica* D **135** 154
Scovel C, Kevrekidis I G and Nicolaenko B 1988 *Phys. Lett.* A **130** 73
[19] Kivshar Yu S, Pelinovsky D E, Cretegny T and Peyrard M 1998 *Phys. Rev. Lett.* **80** 5032
[20] Johansson M and Kivshar Yu S 1999 *Phys. Rev. Lett.* **82** 85
[21] Kevrekidis P G, Bishop A R and Rasmussen K Ø 2001 *Phys. Rev.* E **63** 036603
[22] van der Meer J-C 1990 *Nonlinearity* **3** 1041
[23] Balmforth N J, Craster R V and Kevrekidis P G 2000 *Physica* D **135** 212

[24] Kevrekidis P G and Jones C K R T 2000 *Phys. Rev.* E **61** 3114
[25] Kapitula T, Kevrekidis P G and Jones C K R T 2001 *Phys. Rev.* E **63** 036602
[26] Jordan R, Turkington B and Zirbel C 2000 *Physica* D **137** 353
[27] Novikov S P 1975 *Funct. Anal. Appl.* **8** 236
[28] Kaup D J private communication
[29] Afanasjev V V, Malomed B A and Chu P L 1997 *Phys. Rev.* E **56** 6020
[30] Kevrekidis P G 2001 *Phys. Rev.* E **64** 026611
[31] Kevrekidis P G and Kapitula T unpublished